Supporting Information

Bimetallic Metal-Organic Frameworks: Enhanced Peroxidase-like Activities for Self-activated Cascade Reaction

Xiaoping Zhao,[a] Ning Zhang,[a] Tingting Yang,[a] Daomeng Liu,[a] Xunan Jing,[c] Daquan Wang,[a] Zhiwei Yang, [d] Yunchuan Xie,[a] Lingjie Meng[a,b]*

[a]School of Chemistry, Xi'an Key Laboratory of Sustainable Energy Material Chemistry, Xi'an Jiaotong University, Xi'an 710049, P. R. China

[b]Instrumental Analysis Center of Xi'an Jiaotong University, Xi'an 710049, P. R. China.

[c]Talent Highland, The First Affiliated Hospital, Xi'an Jiaotong University, Xi'an, 710061, China.

[d]MOE Key Laboratory for Nonequilibrium Synthesis and Modulation of Condensed Matter, School of Physics, Xi'an Jiaotong University, Xi'an 710049, China

*Corresponding Author: menglingjie@mail.xjtu.edu.cn

EXPERIMENTAL SECTION

Materials and Reagents. N,N-dimethylformamide (DMF) was purchased from Tianjin Fuyu Fine Chemical Co., Ltd. $FeCl_3 \cdot 6H_2O$ and ethanol were gotten from Sinopharm

Chemical Reagent Co., Ltd. $Ni(NO_3)_2 \cdot 6H_2O$ was obtained from Energy Chemical. Glutathione (GSH), 6-mercapto-1-hexanol (MCH) and 3,3',5,5'-tetramethylbenzidine (TMB) were from Aladdin Industrial Corporation. Glucose (Glu) and glucose oxidase (GOx) were purchased from Sangon Biotech. 1,4-dicarboxybenzene (BDC, TA) and $K_3Fe(CN)_6$ were obtained from Macklin Biochemical Co., Ltd. Nafion and Methyl red were obtained from Sigma and Tianjin Tianxin Fine Chemical Industry Development Center, respectively. 2,' 7'-dichlorofluorescein diacetate (DCFH-DA), Calcein-AM and propidium iodide (PI) were obtained from Beyondtime Bio-Tech. All chemicals were used as received without further purification. All solutions were prepared using ultrapure water (18.2 M Ω·cm) from the Millipore Elix 5 Pure Water System (Purelab Classic Corp., USA).

Characterization and Instruments. Field emission scanning transmission electron microscopy (FESEM, GeminiSEM500, Zeiss), transmission electron microscope (TEM, JEM-2100, JEOL), Lorenz Transmission Electron Microscope (Talos F200X，America，Thermo)) and an energy dispersive X-ray spectroscopy (EDS) was used to characterize the prepared MOFs morphology. The selected area electron diffraction (SAED) pattern was perform on transmission electron microscope (TEM, Thermo, HT (300kV), electron dose (0.28 $e^-/Å^2$), beam current (beam current 1pA)). The valence states and interactions of elements in MOFs was characterized by X-ray photoelectron spectroscopy (XPS, Xi+, Thermo Fisher Scientific). Fe and Ni content in MOFs were determined using inductively coupled plasma mass spectrometer (ICP-MS,NexION 350D, Perkin Elmer). Zeta potentials were performed by a Nano

ZS90 Zeta sizer (Malvern). UV-vis absorbance was recorded on a UV-vis spectrophotometer (Lambda950, Perkin Elmer). The electrochemical detection was performed on an electrochemical workstation (CHI 660E, Chenhua). The molecular change during cell death process were recorded by Raman spectroscopy (HR Evolution, Horiba). Cell viability was measured by MTT experiments on a microplate spectrophotometer (Spectra Max 190, Molecular Devices). Fluorescent images of cells was observed by the inverted fluorescence microscope (Leica DMi8-M, GER).

The structure information of MIL-101: The Cambridge Crystallographic Data Centre (CCDC, Deposition Number: 605510；

OCUNAC:catena-[tris(μ4-Terephthalato)-(μ3-oxo)-diaqua-fluoro-tri-chromiumpentadecahydrat]; Space Group: Fd3m (227); Cell: a 88.86899Å b 88.86899Å c 88.86899Å, α 90° β 90° γ 90°; Associated publication: Science, 2005, 309, 2040.

X-ray diffraction (XRD): XRD patterns were collected on a X-ray diffractometer using Cu–Kα radiation (D8 Advances, Bruker). The details of the experiment parameter is as follow: 2θ=4-30°; step size: 0.02(2θ); time acquisition/step: 0.1 s ; λ = 1.5418 Å; operating voltage=40 kV; current=40 mA; d-spacing (d)= was calculated using $2d\sin\theta=\lambda$.

Small angle X-ray scattering (SARS): Small angle X-ray scattering (SARS) patterns were obtained on a Small angle X-ray scattering instrument using Cu–Kα radiation (Anton Paar, SAXS point 2.0). The details of the experiment parameter is as follow: λ = 1.5418 Å; operating voltage=50 kV; current=1mA; Height:120mm; Acquisition time: 10min ; Scattering angles (θ) were calculated from scattering vectors (q) using

$q=4\pi\sin\theta/\lambda$, and d-spacing (d) was calculated from the principal scattering maxima (q) using $d=2\pi/q$.

Nitrogen adsorption-desorption: Nitrogen adsorption-desorption isotherms were carried out by standard volumetric techniques (ASAP 2460 Version 2.02) at -195.8 °C (degassing temperature at 100 °C, 150 °C or 200 °C for 8 h). BET surface area and pore size distribution can be obtained by attained isotherms. The details of the experiment parameter is as follow: Analysis adsorptive: N_2; Analysis bath temp.: -195.8 °C; Sample mass: 0.096 g; Warm free space: 28.37 cm^3 Measured; Cold free space: 84.2 cm^3; Equilibration interval: 10 s; Sample density: 1.0 g/cm^3. BET surface area and pore size distribution can be obtained by attained isotherms.

The Mössbauer measurements were measured at room temperature using a conventional spectrometer (Germany, Wissel MS-500) in transmission geometry with constant acceleration mode. A 57Co(Rh) source with activity of 25 mCi was used. The velocity calibration was done with a room temperature α-Fe absorber.

Cell Culture. HeLa cells were first dispersed in Dulbecco's Modified Eagle's Medium (DMEM) containing10% fetal bovine serum (FBS), 100 U/mL penicillin, and 100 μg/mL streptomycin, and then placed an incubator containing 5% CO_2 at 37 ˚C.

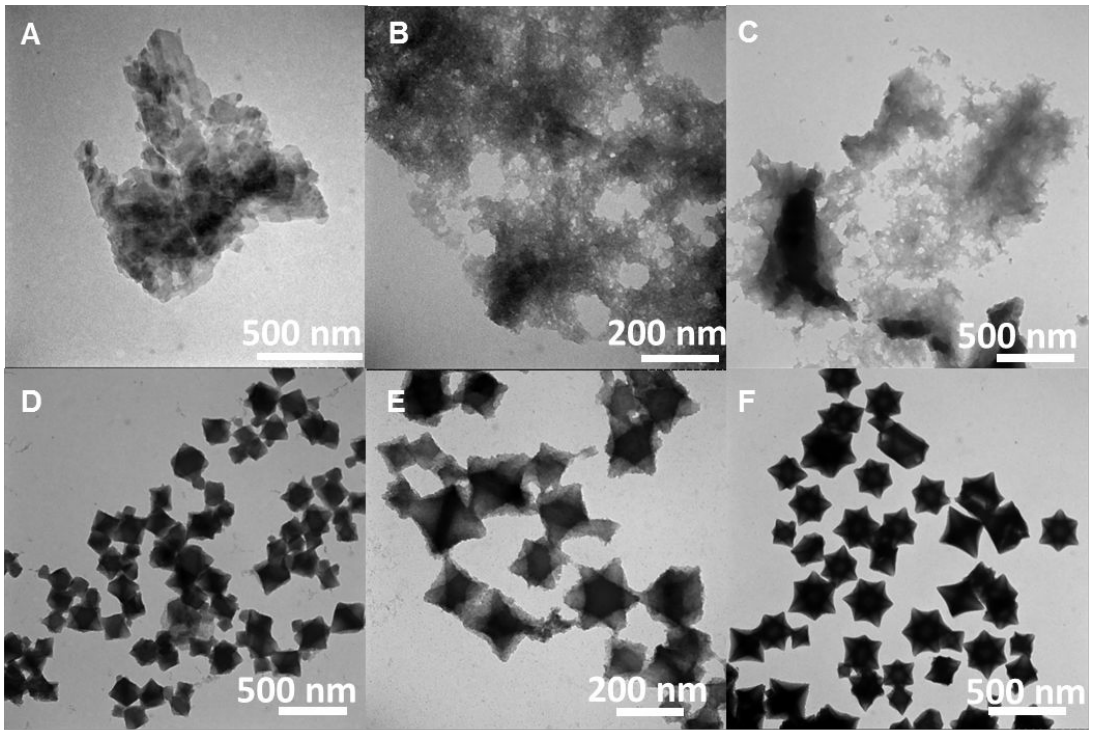

Figure S1. TEM images of (A) Ni-MOF, (B) Ni_2Fe-MOF, (C) NiFe-MOF, (D) $NiFe_2$-MOF, (E) $NiFe_3$-MOF, and (F) Fe-MOF.

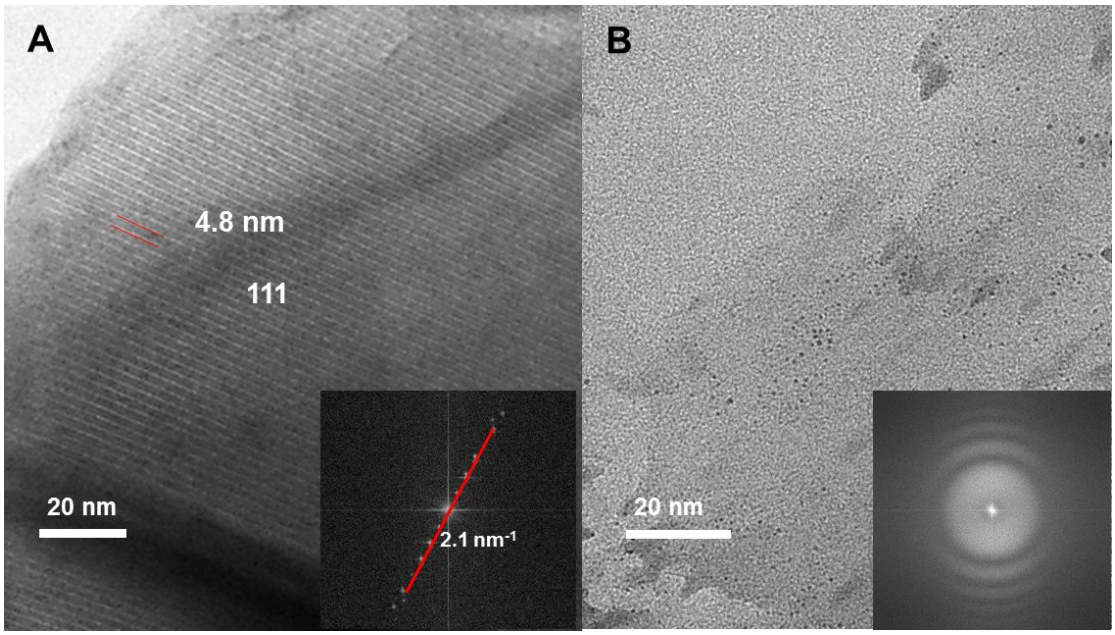

Figure S2. HRTEM image of Fe-MOF (A), the inset is the corresponding FFT. HRTEM image of Ni-MOF (B), the inset is the corresponding FFT.

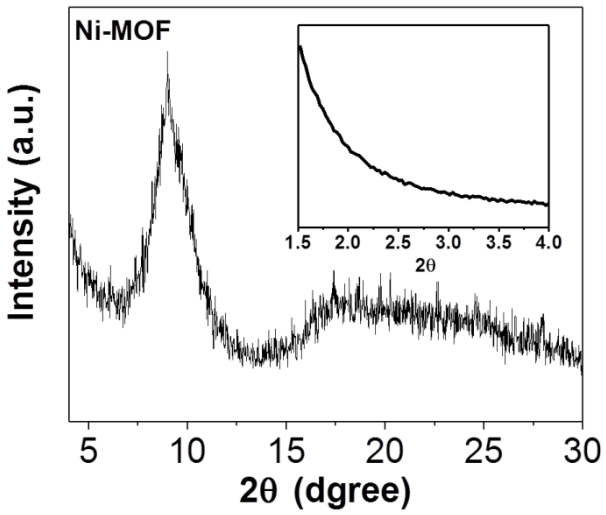

Figure S3. X-ray diffraction (XRD) patterns of Ni-MOF. Small angle X-ray scattering (SAXS) patterns of Ni-MOF at 1.5˚-4˚.

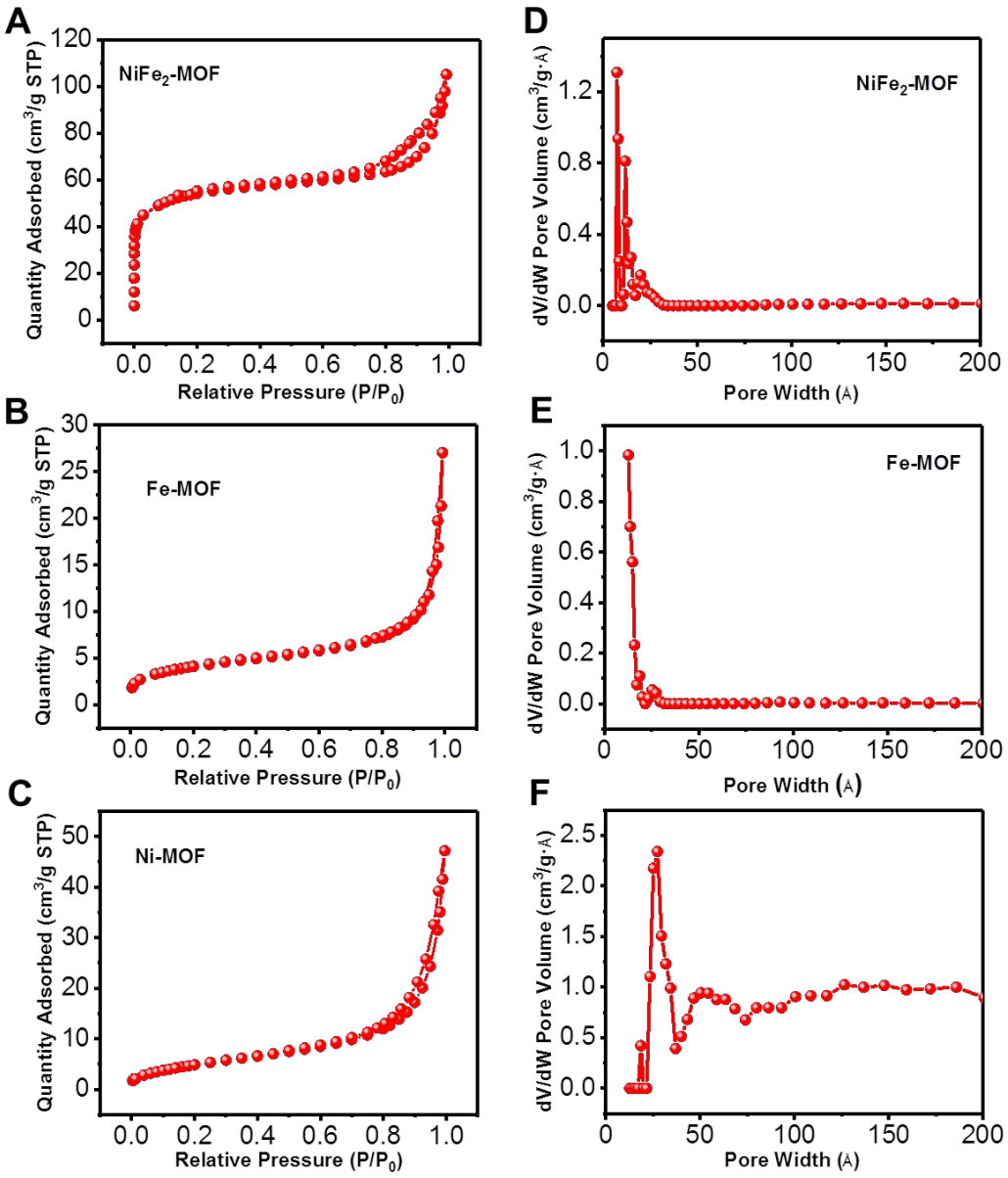

Figure S4. (A-C) N_2 adsorption–desorption isotherms and (D-F) pore size distribution of different MOFs (BJH method).

Table S1. Surface area of Fe-MOF and $NiFe_2$-MOF at different degassed temperature.

Surface area (m^2/g) / Degassed Temperature (°C)	Fe-MOF	$NiFe_2$-MOF
100	29.563	178.24
150	239.21	355.78
200	138.54	274.12

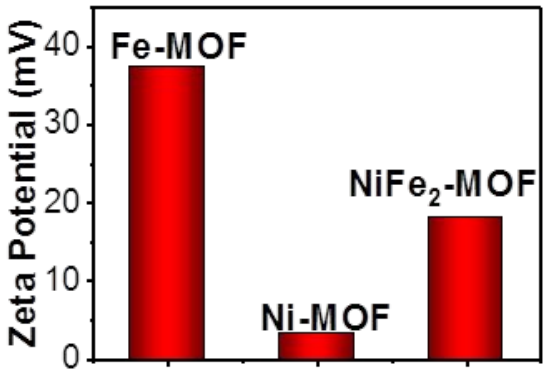

Figure S5. Zeta potentials of Fe-MOF, Ni-MOF, and $NiFe_2$-MOF.

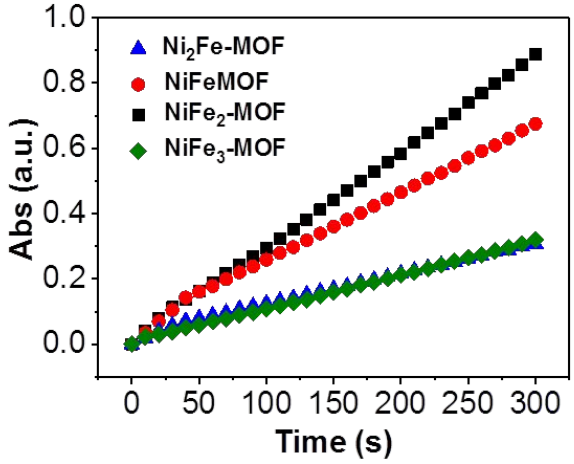

Figure S6. The peroxidase-like activity of different catalysts in TMB/H_2O_2 solution with pH 4.5 at room temperature for 6min.

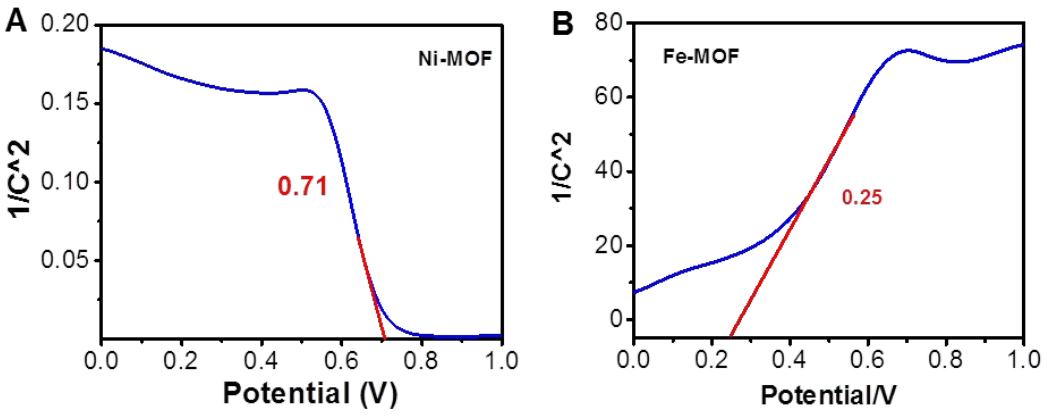

Figure S7. Mott-Schottky plots of Ni-MOF (A) and Fe-MOF (B).

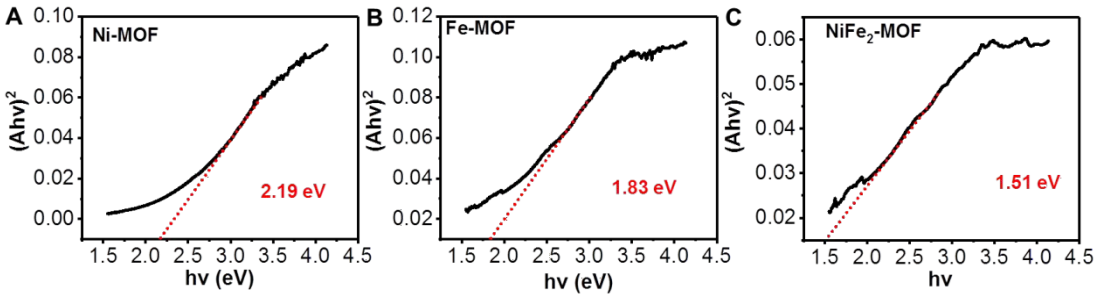

Figure S8. The optical bandgap of Ni-MOF(A), Fe-MOF(B) and $NiFe_2$-MOF (C).

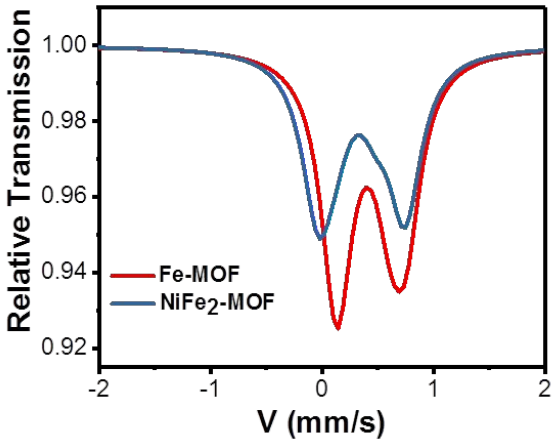

Figure S9. M¨ossbauer transmission spectra of Fe-MOF and $NiFe_2$-MOF.

Table S2. Compared K_m and V_{max} between the $NiFe_2$-MOF, other nanozymes and HRP.

	K_m (mM)		V_{max}(10^{-8}M.s^{-1})	
Catalyst	TMB	H_2O_2	TMB	H_2O_2
HRP[1]	3.759	11.63	2.758	1.411
MIL-53(Fe)[2]	1.08	0.04	8.78	1.86
Fe-MIL-88NH_2 [3]	2.84	2.06	10.47	7.04

CuNPs@C [4]	1.65	1.89	12.05	5.30
Fe-Co alloy NPs [5]	1.79	0.06	4.56	1.32
PVP-CoNPs [6]	5.09	1.14	9.98	1.72
MOF(Co/2Fe) [7]	0.25	4.22	3.78	4.91
$NiFe_2$-MOF	0.71	0.066	16.7	5.43

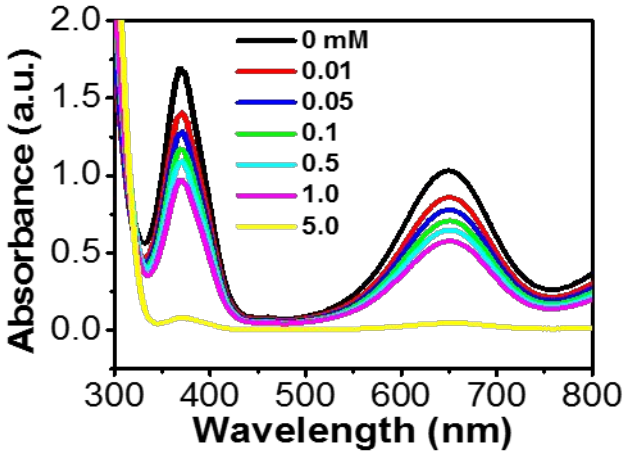

Figure S10. UV-vis spectra of TMB/$NiFe_2$-MOF/H_2O_2 after adding different concentration of GSH for 5min. GSH concentration: 0.01 mM, 0.05 mM, 0.1 mM, 0.5 mM, 1.0 mM, 5.0 mM.

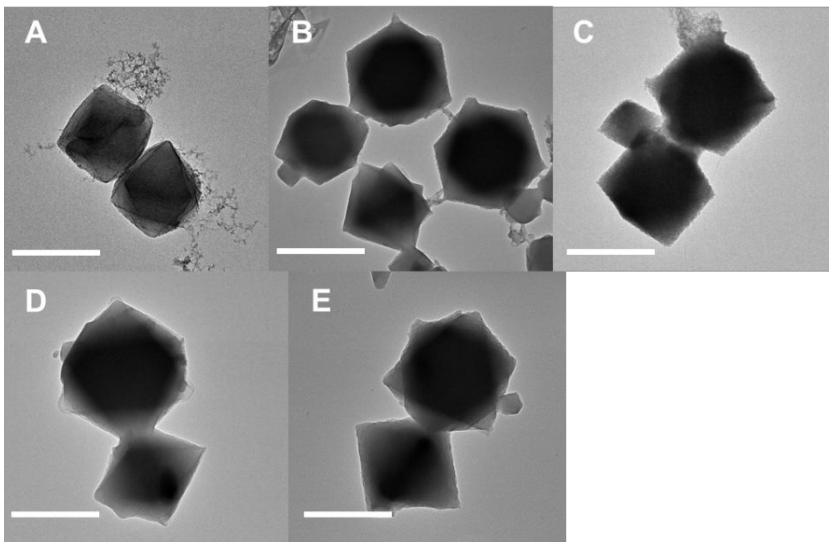

Figure S11. TEM image of $NiFe_2$-MOF at different pH. (A) pH 3.5; (B) pH 4.5; (C)

pH 5.5; (D) pH 6.5; (E) pH 7.4. Scale Bar=200 nm.

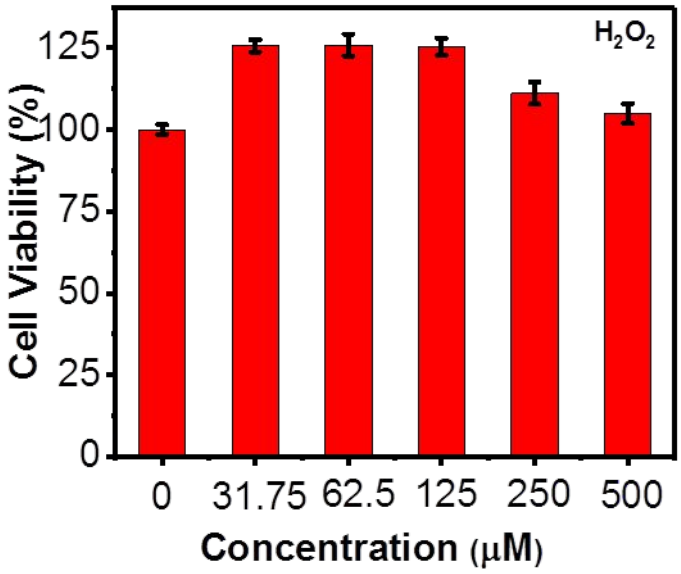

Figure S12. Cell viability of HeLa cells culture by various concentrations of H_2O_2.

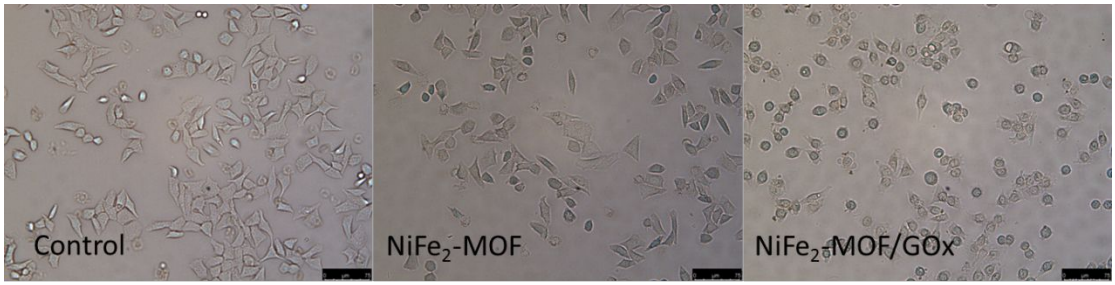

Figure S13. The microscope image of HeLa cells morphology after incubation with free medium, $NiFe_2$-MOF (10 μg/mL) and $NiFe_2$-MOF/GOx (10 μg/mL) for 2h. Scale Bar=75μm.

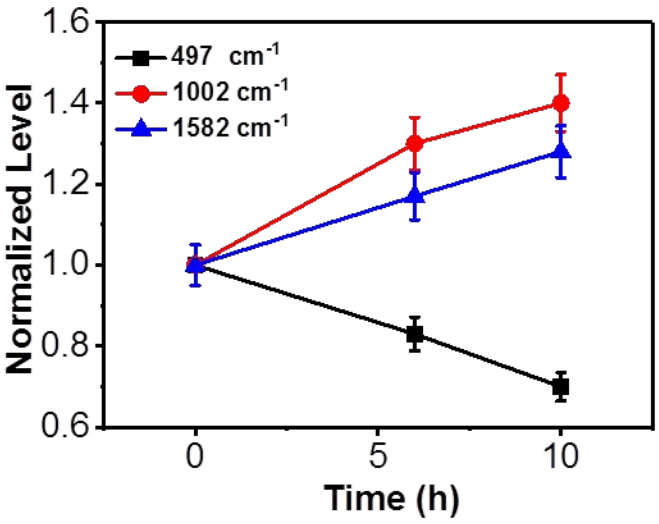

Figure S14. The relative change of Raman intensities at 497, 1002 and 1582 cm^{-1} during chemo-dynamic process.

REFERENCE

(1) Xu, B.; Wang, H.; Wang, W.; Gao, L.; Li, S.; Pan, X.; Wang, H.; Yang, H.; Meng, X.; Wu, Q.; Zheng, L.; Chen, S.; Shi, X.; Fan, K.; Yan, X.; Liu, H. A Single-Atom Nanozyme for Wound Disinfection Applications. *Angew. Chem.* **2019**, *131*, 4965-4970.

(2) Ai, L.; Li, L.; Zhang, C.; Fu, J.; Jiang, J. MIL-53(Fe): A Metal–Organic Framework with Intrinsic Peroxidase-Like Catalytic Activity for Colorimetric Biosensing. *Chem. Eur. J.* **2013**, *19*, 15105 -15108.

(3) Liu, Y. L.; Zhao, X. J.; Yang, X. X.; Li, Y. F. A Nanosized Metal-Organic Framework of Fe-MIL-88NH_2 as a Novel Peroxidase Mimic Used for Colorimetric Detection of Glucose. *Analyst* **2013**, *138*, 4526-4531.

(4) Tan, H.; Ma, C.; Gao, L.; Li, Q.; Song, Y.; Xu, F.; Wang, T.; Wang, L.

Metal-Organic Framework-Derived Copper Nanoparticle@Carbon Nanocomposites as Peroxidase Mimics for Colorimetric Sensing of Ascorbic Acid. *Chem. Eur. J.* 2014, *20*, 16377-16383.

(5) Mu, J.; He, Y.; Wang, Y. Copper-Incorporated SBA-15 with Peroxidase-Like Activity and Its Application for Colorimetric Detection of Glucose in Human Serum. *Talanta* 2016, *148*, 22-28.

(6) Chen, Y.; Cao, H.; Shi, W.; Liu, H.; Huang, Y. Fe-Co Bimetallic Alloy Nanoparticles as a Highly Active Peroxidase Mimetic and Its Application in Biosensing. *Chem. Commun.* 2013, *49*, 5013-5015.

(7) Yang, H.; Yang, R.; Zhang, P.; Qin, Y.; Chen, T.; Ye, F. A Bimetallic (Co/2Fe) Metal-Organic Framework with Oxidase and Peroxidase Mimicking Activity for Colorimetric Detection of Hydrogen Peroxide. *Microchim. Acta.* 2017, *184*, 4629-4635.